

# Time-dependent material modeling for finite element analyses of flip chips

Frank Feustel, Steffen Wiese, Ekkehard Meusel

Dresden University of Technology, Semiconductor & Microsystems Technology Laboratory

TU Dresden, IHM, D-01062 Dresden, Germany

feustel@ihm.et.tu-dresden.de

## Abstract

Finite element analyses (FEA) have established as effective method for reliability assessment of flip chip assemblies. The simulation results are significantly dependent on the selected material models. Regarding flip chip assemblies, this statement mainly applies to the tin lead solder of the flip chip joints and the encapsulant – the so-called underfill.

Comprehensive material data of eutectic solder were determined on real flip chip joints by TU Dresden. Based on these data three modeling approaches were evaluated (target platform was the FEA code ANSYS): viscoplasticity (Anand's model), power law creep (with 2 terms) + plasticity, and sinh law creep + plasticity (as user defined model in ANSYS).

Underfills are often modeled as very simple elastic materials. Tensile tests were performed on underfill samples to study its real behavior. Two modeling approaches of a representative underfill were evaluated: linear elasticity and linear viscoelasticity.

The properties of all above mentioned approaches are discussed in terms the simulated material behavior at various temperatures and deformation rates. For each combination of approaches, temperature cycling tests on a flip chip module were simulated by ANSYS. Different combinations of modeling approaches for solder and underfill led to different simulation results although each model was based on the same measurement data. The differences are discussed and conclusions are drawn which modeling approach is preferable for typical applications.

## Introduction

Finite element simulations have established as effective tool for thermo-mechanical reliability assessment of electronic assemblies. The simulation results are influenced by the material models that are used. Both, solder and underfill are characterized by a deformation behavior which is dependent on temperature and deformation rate, i.e. time. Tin lead solder has been the object of studies for a longer time. At TU Dresden, comprehensive material data were determined on real flip chip joints. However, many sources of material data differ from each other. Moreover, there is no uniform modeling approach that is commonly accepted.

The availability of data of representative underfill materials is much poorer than compared with solder. Moreover, underfills are often modeled as very simple elastic materials. Only part of recent publications considers a dependence on temperature. Almost no publication considers a dependence on deformation rate (i.e. time). However, the material structure (epoxy based polymer) indicates a deformation behavior that is dependent on both, temperature and time.

The objective of this work was to study different modeling approaches of solder and underfill, to derive influences of the

material model on the simulation results, and to draw conclusions, which modeling approach is preferable for typical applications.

## Deformation behavior of solder in flip chip scale

### Experiments

Most of the material data that was published for eutectic SnPb solder, e.g. [1-3], was determined on specimens having a volume between  $V = (10^{-10} \dots 10^{-6}) \text{ m}^3$ . Since flip chip solder joints have a significant smaller Volume  $V < 10^{-12} \text{ m}^3$ , there was a lot of doubt if bulk specimen data is valid for the flip chip scale of the solder material. Therefore, shear tests on real flip chip joints were carried out. These experiments are detailed described in [4,5]. Briefly, a flip chip specimen was designed consisting of two identical silicon chips bonded against each other by four flip chip solder joints (each on one corner). A test setup was realized that is able to impose simple shear on the flip chip specimen with strain rates between  $\dot{\epsilon} = (10^{-7} \dots 10^2) \text{ s}^{-1}$ . The measurement resolution is 2 nm for displacement and 1 mN for force. The experimental loading conditions consisted of constant stress (creep) and a cyclic triangular strain wave (constant strain rate). Comprehensive information about the entire experimental program is given in [5].

### Solder constitutive modeling

Since the flip chip joint has a very complex geometry the stress-strain relations could not be derived by simple analytical relations. Therefore, an iterative FEA of the shear experiments was carried out in order to determine the parameters of the solder constitutive models in ANSYS. For all the iterative FE analysis, which are described in [4], version 5.3 of the ANSYS software package was used. A half flip chip solder joint was modeled by 500 elements. Element types were either Solid92 (+ user defined creep model if necessary) or Visco107. In case of the evaluation of cyclic experiments, always the initial and the subsequent cycle was simulated.

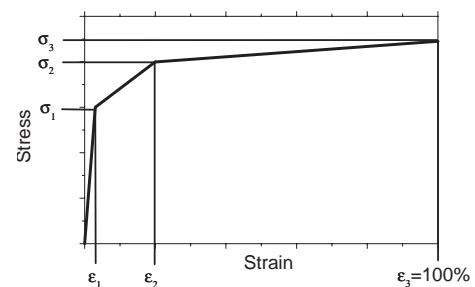


Fig. 1: Elastic plastic model

The most effective model, which showed good fitting capability consisted on a dual description divided into an elastic-

plastic model and a creep model. The time independent elastic-plastic description is characterized by 5 parameters ( $\sigma_1, \sigma_2, \sigma_3, \epsilon_1, \epsilon_2$ ). The model (Fig.1, Tab.1) uses the multilinear kinematic hardening model of ANSYS. It is composed of 3 adjoining lines starting in the origin.

Par.	$\epsilon_1$	$\epsilon_2$	$\sigma_1$	$\sigma_2$	$\sigma_3$	$E$
Unit	—	—	MPa	MPa	MPa	GPa
280K	7e-4	3e-3	21	41	600	29
320K	7e-4	3e-3	19	31	200	

Table 1: Parameters of the elastic-plastic model for SnPb37 solder in flip chip scale

For the steady state creep model two alternative models - the sinh law model (Eq. (1)) and the double power law model (Eq. (2)) - were implemented. The sinh law model does not come along with the ANSYS software and has to be implemented as a so-called user defined model (modifications in source code).

$$\dot{\epsilon} = C_1 \cdot [\sinh(C_3 \cdot \sigma)]^{C_2} \cdot \exp\left(-\frac{C_4}{T}\right) \quad (1)$$

However, equation (1) is already included in the Anand's model for viscoplastic elements, where the Parameters  $C_1 \dots C_4$  correspond with  $A, 1/m, \xi/s, Q/k$ . The parameter  $h_0$  must be set to zero in order to skip all evolution equations, because SnPb37 Solder does not undergo cyclic hardening.

Anyway, one should pay attention, that viscoplastic elements do model only elasticity and steady state creep but no plasticity, which leads to increasing errors when deformations are little or strain rates are high.

Par.	$C_1$	$C_2$	$C_3$	$C_4$	$\sigma$	$T$	$\dot{\epsilon}$
Unit	s <sup>-1</sup>	—	MPa <sup>-1</sup>	K	MPa	K	s <sup>-1</sup>
Value	10	2	0.2	5400	—	—	—

Table 2: Parameters of the sinh law model (Eq. (1)) for SnPb37 solder in flip chip scale

The disadvantages of either writing a user defined model or the absence of plastic behavior in the Anand's model can be overcome by using the double power law model (Eq. (2)).

$$\dot{\epsilon} = C_1 \cdot \sigma^{C_2} \cdot \exp\left(-\frac{C_3}{T}\right) + C_4 \cdot \sigma^{C_5} \cdot \exp\left(-\frac{C_6}{T}\right) \quad (2)$$

Equation 2 consists on two power law terms which need to be separately implemented into ANSYS by using parameters of a primary and a secondary creep model.

Par.	$C_1$	$C_2$	$C_3$	$C_4$	$C_5$	$C_6$	$\sigma$	$T$	$\dot{\epsilon}$
Unit	s <sup>-1</sup>	—	K	s <sup>-1</sup>	—	K	MPa	K	s <sup>-1</sup>
Value	0.4	2	5400	21	7	9500	—	—	—

Table 3: Parameters of the double power law model (Eq. (2)) for SnPb37 solder in flip chip scale

## Deformation behavior of underfill

### Measurement results

Underfill is a polymer based compound material. Therefore it is supposed to have a deformation behavior which is dependent

on temperature and time. Underfill specimen with a strip shape were prepared and subjected to tensile tests. The tests were performed at three temperatures which were derived from typical temperature cycle tests: 23°C, 80°C, and 125°C. A reduced influence of temperature and time was expected at lower temperatures than 23°C therefore no tests were done below that. The strain rates that were applied were also derived from typical temperature cycles tests:  $2 \cdot 10^{-3} \text{ s}^{-1}$ ,  $2 \cdot 10^{-4} \text{ s}^{-1}$ , and  $2 \cdot 10^{-5} \text{ s}^{-1}$ . Corresponding times range from some seconds to approx. 15 minutes. A finite element analysis was used to estimate the required maximum strain of (0.5...1)%. A final strain of 2% was used during the tensile tests.

As result of the experiments, stress-strain diagrams were obtained as shown in Fig. 2. They are characterized by a strong dependence on temperature. At 125°C, there is an additional dependence on strain rate. Similar results were published e.g. in [6]. From the stress-strain diagrams, the development of the tensile modulus versus time can be calculated. At 23°C and 80°C, the same curve is obtained at any time. At 125°C, the tensile modulus decreases with time (Fig. 3), i.e. the underfill material shows relaxation. The modulus is only dependent on time unless more than approx. 0.4% strain is reached. The underfill has the characteristics of a linear viscoelastic material.

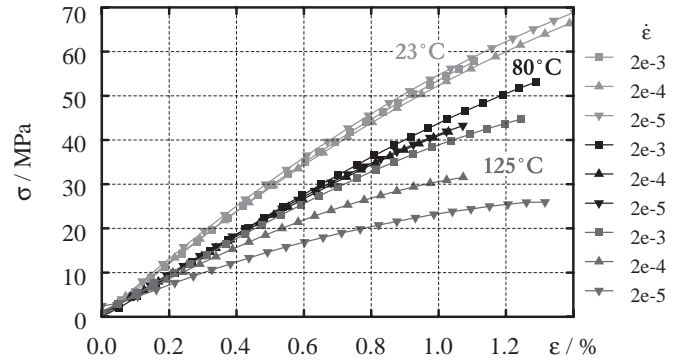


Fig. 2: Stress-strain diagram of the underfill

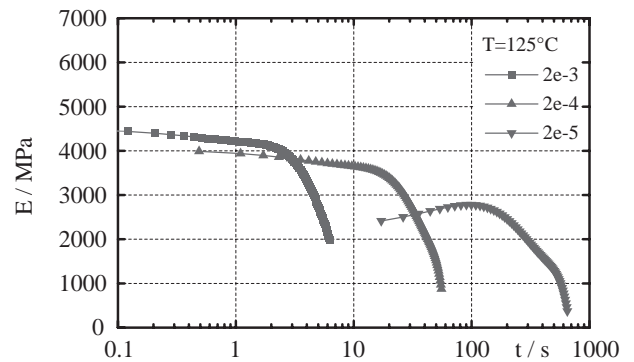


Fig. 3: Development of the tensile modulus versus time

### Material modeling

Target of the material modeling was the FEA code ANSYS which offers a variety of possible approaches (Tab. 4). Satisfactory results could only be achieved using a linear-elastic and a linear-viscoelastic model.

Model approach	Example element	Dependence on		
		temp.	time	stress
linear elastic	Plane82	■	—	—
elastic-plastic	Plane82	■	—	■
viscoplastic	Visco108	■	■	■
lin. viscoelastic	Visco88	■	■	—

Table 4: Modeling approaches

A linear elastic model is the simplest approach for the underfill material. It is characterized by only one parameter, the Young's modulus  $E$ , which was determined from the measurement data by a linear regression of the stress-strain curve within the interval of (0...1)% strain. The slope of the resulting line was considered as  $E$ . At 125°C, the regression line of the stress-strain curve that represents the slowest strain rate of  $2 \cdot 10^{-5} \text{ s}^{-1}$  was used to avoid too optimistic simulation results. Table 5 shows the parameters of the linear-elastic underfill model.

Temperature $T / ^\circ\text{C}$	23	80	125
Young's modulus $E / \text{MPa}$	5600	4500	2300

Table 5: Parameters of the linear-elastic underfill model

A linear-viscoelastic model is an extension of the elastic model by consideration of time dependent deformation behavior. In ANSYS, viscoelastic behavior is described by a generalized MAXWELL model. The tensile modulus, which is dependent on time and temperature, is given by Eq. 3 and Eq. 4.

$$E(t) = \sum_{i=1}^n E_i \cdot e^{-t/\tau_i} + E_\infty \quad (3)$$

$$\tau_i = \tau_{i0} \cdot e^{H/(R_0 T)} \quad (4)$$

Eq. 3 describes the so-called master curve at a reference temperature  $T_{ref}$ . In this study, 80°C was chosen as reference temperature. The measured modulus-time curve at 80°C was taken over into the master curve without changes. The measured curves at 125°C and 23°C were stretched or compressed, respectively, by a time factor. Afterwards, all curves were combined to the complete master curve of the underfill (Fig. 4). The activation energy  $H$  was calculated from the time factor by Eq. 4 which gave  $H = 130 \text{ kJ/mol}$ . The curve fit of the measured master curve according to Eq. 3 gave the parameters of the MAXWELL model. The use of three MAXWELL elements proved to be sufficient. Tab. 6 shows the parameter input for the ANSYS elements Visco88/89.

$H/R_0$	$E_0$	$E_\infty$	$C_1$	$\tau_1$
15644	5630	1300	0,264	0,198
$C_2$	$\tau_2$	$C_3$	$\tau_3$	
0,200	451	0,536	30435	

Table 6: Parameters of the viscoelastic underfill model ( $H/R_0 / \text{K}$ ,  $E_i / \text{MPa}$ ,  $\tau_i / \text{s}$ )

Parameter  $E_\infty$  cannot be derived from the measurement results. It was assumed to be the lowest value of  $E$  within the relevant interval:  $E(T = 125^\circ\text{C}, \dot{\epsilon} = 2 \cdot 10^{-5} \text{ s}^{-1}, t = 500 \text{ s})$ .

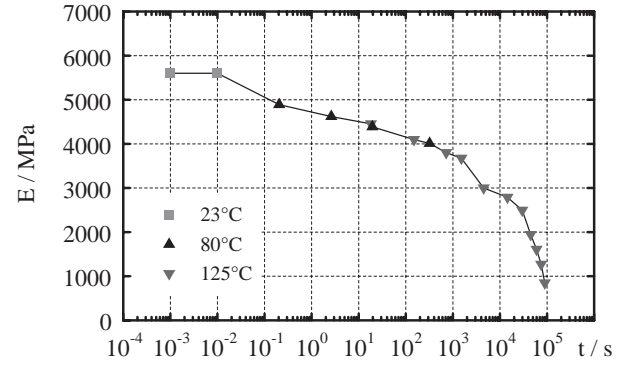


Fig. 4: Master curve of the underfill

The validation of the model was done by simulating the previously performed tensile tests with ANSYS. The calculated force-displacement curves are in very good agreement with the experimental data (Fig. 5).

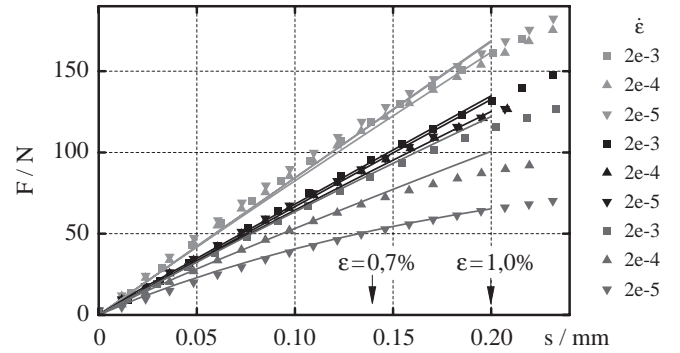


Fig. 5: Comparison of measurement and simulation

The CTE of the studied underfill was measured as 25 ppm/K using a video technique [7].

## Thermo-mechanical simulation

### Geometry model

The geometry of the finite element model is based on a real flip chip assembly which is typically used by TU Dresden for technological studies. Details are described in [8]. The chip (TC1) has an edge length of 7.2 mm and a thickness of 500 μm. Electroplated bumps of eutectic solder are arranged along the perimeter of the chip. The substrate consists of 1 mm thick FR-4 with a Cu/Ni/Au metallization which has a total thickness of 25 μm. The chip stand-off is 75 μm.

The geometry of the assembly is represented by a 2D model. It contains only one half of the flip chip. Appropriate symmetry conditions were defined along the cut through the center of the chip. Fig. 6 shows the region of the solder joint in the model.

The geometry model was meshed with different types of ANSYS elements depending on the used approach for the material modeling of solder and underfill (Tab. 7 and 8). The total number of elements was 1384 of which 312 fell to the solder and 490 to the underfill.

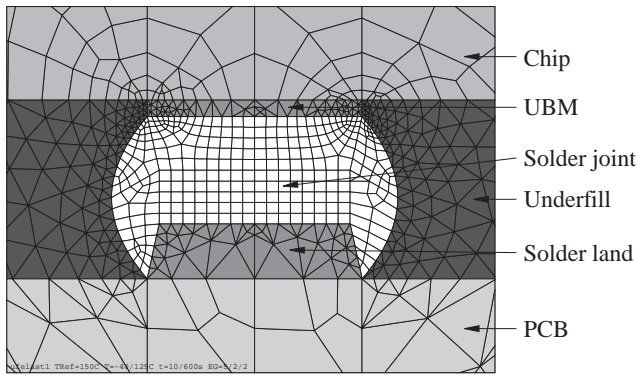


Fig. 6: Section of the geometry model

solder model	plastic	d. power	Anand's	sinh
element type	Plane82	Plane82	Visco108	Plane82 <sup>a</sup>

Table 7: Element types used for solder

a. with user-defined creep equation

underfill model	linear elastic	linear viscoelastic
element type	Plane82	Visco88

Table 8: Element types used for underfill

#### Load model

The load model represents a temperature cycle test from  $(-40 \dots +125)^\circ\text{C}$ . Additionally, a reduced temperature interval  $(0 \dots 80)^\circ\text{C}$  was considered comprising only half of the above range but having the same mean temperature. The starting temperature of all simulations was  $150^\circ\text{C}$  as this represents typical curing conditions of underfill. At the same time, this was the reference temperature at which the flip chip assembly was considered as stress-free. The temperature transitions were described by exponential functions in the form of  $T \sim e^{-t/\tau}$ . Two different transition times were used: 180s as typical value and 10s as very fast transition. The total time of one cycle was 1200s. The temperature distribution was assumed as homogeneous across the complete assembly. Fig. 7 shows the first of three cycles that were simulated.

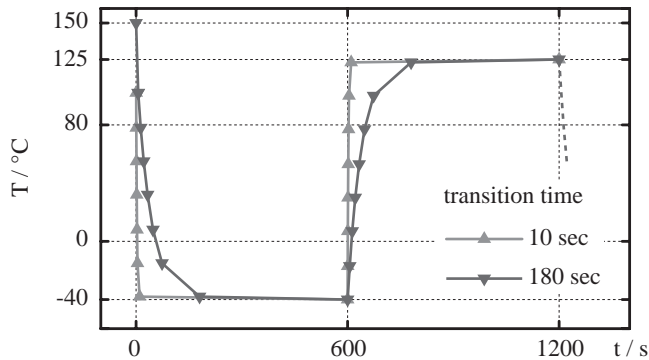


Fig. 7: Load model: temperature cycle test

#### Evaluation criteria

Any temperature change leads to a warpage of the flip chip assembly. It could be demonstrated in [9] that this is the fundamental mechanism of solder joint protection. Thermally in-

duced stresses occur in all parts of the assembly. The following quantities were selected as criteria to evaluate the stress situation and the lifetime expectation:

- A) chip warpage  $u_{y \text{ chip}}$   
deflection of the chip edge vs. the chip center
- B) solder strain  $\epsilon_{cr \text{ acc}}$   
accumulated creep strain per cycle in a deformation band that reaches across the whole solder joint (Fig. 9)
- C) underfill delamination stress  $\sigma_{delami}$   
stress at the interface chip-underfill next to a solder joint

Especially quantity C is rather mesh-dependent due to singularities that occur at edges and notches. Therefore, all simulations used the same mesh that the calculated stresses can be compared and considered as indicator of the delamination risk.

#### Comparison of results: solder models

Three different solder models were applied to the solder joints as already described above: sinh law, double power law, and Anand's. As fourth model, an instantaneous plastic model was added which was derived from the sinh/double power law model by disabling all creep properties. The linear elastic model was assumed for the underfill to avoid any superpositioning effects that are generated by nonlinear behavior of the underfill.

The chip warpage  $u_{y \text{ chip}}$  did not show any dependence on the solder model (Fig. 8). Obviously, the solder joints have no influence on the global deformation behavior which is dominated by chip, substrate, and underfill.

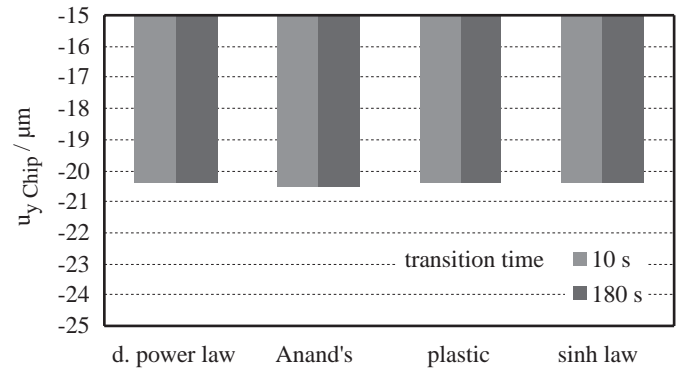


Fig. 8: Chip warpage  $u_{y \text{ chip}}$  at  $-40^\circ\text{C}$  (underfill model: elastic)

Significant differences were obtained in terms of the calculated strain in the solder joint. The plastic model generated almost no inelastic strains. This behavior results from the fact that the assembly is almost stress-free at the upper temperatures of the cycle test when the plastic model has its lowest yield stress. At lower temperatures, the thermo-mechanical stresses increase but at the same time the yield stress of the plastic model increases. The simulation results of the plastic model do not allow any reasonable estimation of the solder joint reliability.

The sinh law model generated a typical strain distribution in the solder joint (Fig. 9). Approximately 0.4% creep strain are accumulated per cycle (Fig. 10). Plastic deformations are negligible. A dependence on the transition time of the temperature cycle test was not detectable. At the reduced temperature range  $(0 \dots 80)^\circ\text{C}$  (50%  $\Delta T$ ) less than half of the strain is calculated. This result indicates the acceleration effect when testing is done



at  $(-40 \dots +125)^\circ\text{C}$ . Drawbacks of the sinh law model are that long calculation times are needed and a user-defined creep equation has to be defined.

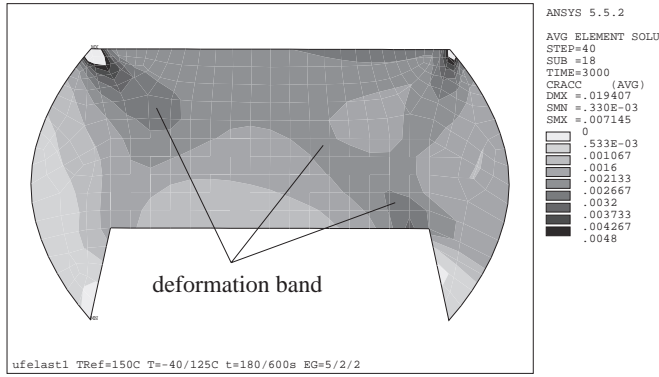


Fig. 9: Typical strain distribution of the sinh law model

The double power law model gave very similar results as the sinh law model. Slightly less strain was calculated at the fast transition time (10s). It requires the same calculation time, however, it has the great advantage that this model approach is already implemented in ANSYS.

The viscoplastic model (Anand's) generated a strain profile that partly differed from the above described, i.e. qualitative differences were obtained by the use of this model. Quantitatively, the Anand's model gave strains that typically were twice as high as with the sinh/double power law models. An influence of the transition time was not detected.

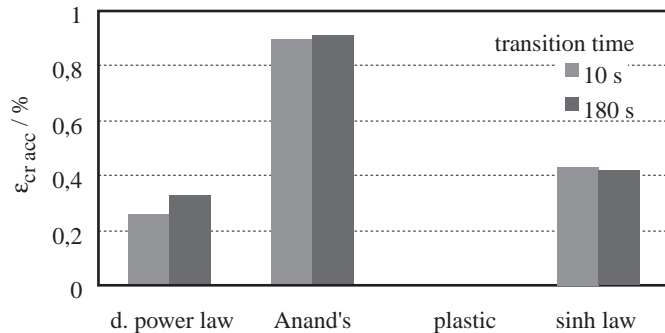


Fig. 10: Solder strain  $\epsilon_{cr acc}$  during the 3rd cycle  $(-40 \dots 125)^\circ\text{C}$  (underfill model: elastic)

The missing dependence on the transition time indicates that the creep rate of the solder models is high enough that stress relaxation takes place as fast as stresses are generated by thermally induced strains. Under these conditions, it appears conceivable to tailor a nonlinear time-independent model (i.e. a plastic model) with effective stress-strain curves that gives comparable results in terms of the time-dependent sinh/double power law models. The gain would be shorter calculation times.

All in all, the sinh law model and the double power law model appear equally good. Both models are proposed for all simulation purposes in the sector of packaging.

### Comparison of results: underfill models

Two different underfill models were applied to the underfill layer as described above: the linear elastic model and the linear viscoelastic model. The sinh law model was used for the solder joint.

The chip warpage  $u_{y chip}$  was determined by the temperature range but not dependent on the transition time. The viscoelastic model generated only slightly more warpage of the chip.

The accumulated creep strain  $\epsilon_{cr acc}$  in the solder joint was significantly higher if the viscoelastic underfill model was used. In comparison to the elastic model, the value approximately doubled. At the reduced temperature range  $(0 \dots 80)^\circ\text{C}$ , less than half of the strain is calculated. This behavior applies to both underfill models.

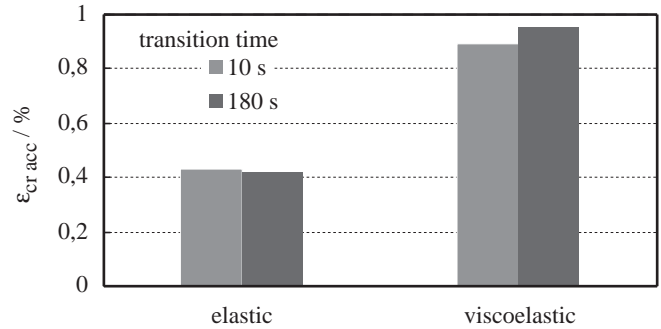


Fig. 11: Solder strain  $\epsilon_{cr acc}$  during the 3rd cycle  $(-40 \dots 125)^\circ\text{C}$  (solder model: sinh law)

The underfill delamination stress  $\sigma_{delami}$  had a similar distribution for both models (Fig. 12). The value of the principal stresses gave some higher results when the viscoelastic model was used. However, significant differences were detected in terms of the triaxiality factor of the stress (Fig. 13). In addition to the stress level, this quantity has a great influence on the propagation of delamination cracks.

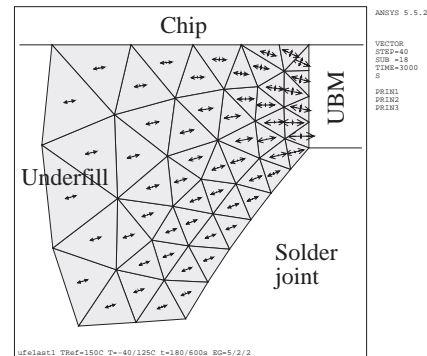


Fig. 12: Typical stress distribution in the underfill at  $-40^\circ\text{C}$

All in all, the linear elastic underfill model distinctly underestimates the solder fatigue and the delamination risk of the underfill. The advantages of the simpler model in terms of the calculation speed are only moderate.

### Conclusions

Different model approaches lead to different FEA results although they are based on the same set of measurement data.

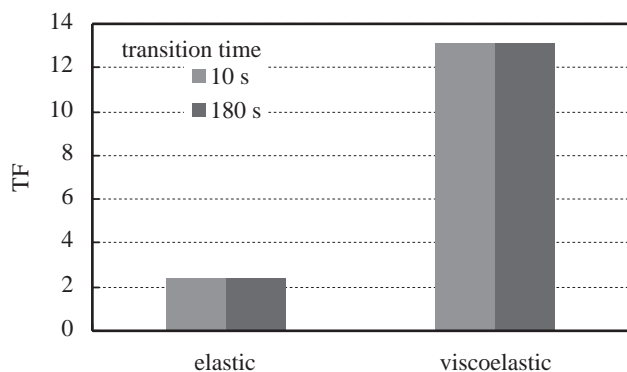


Fig. 13: Maximum triaxiality factor in the underfill at -40°C

The solder model influences the accumulated strains in the joint. Not only quantitative but also qualitative differences, i.e. other strain distributions, are calculated. The sinh law model and the double power law model, which have similar properties, are proposed for application in future simulations. The modeling of the underfill as linear elastic material underestimates the strains in the solder joint and the delamination risk. It is proposed to always use a viscoelastic model approach. However, there is a great lack of material data due to the large variety of commercially available underfills. The chip warpage is not influenced by different model approaches. The significant influence of the time-dependent modeling of the underfill indicates that other parts of the flip chip assembly, e.g. an organic substrate, may require an improved modeling, too.

## References

1. Lam, S. T., Arieli, A., Mukherjee, A. K.: "Superplastic Behavior of Pb-Sn Eutectic Alloy". *Materials Science and Engineering*, 40 (1979), pp. 73–79
2. Shine, M. C., Fox, L. R.: "Fatigue of Solder Joints in Surface Mount Devices". *Low Cycle Fatigue*. Special Technical Publications 942, American Society for Testing and Materials, Philadelphia, 1987, pp. 588–610
3. Darveaux, R., Banerji, K.: "Constitutive Relations for Tin-Based-Solder Joints". *Proc. IEEE 42th Electronic Components and Technology Conference*, 1992, pp. 538–551
4. Wiese, S., Feustel, F., Rzepka, S., Meusel, E.: "Experimental Characterization of Material Properties of 63Sn37Pb Flip Chip Solder Joints". *Electronic Packaging Materials Science X - MRS Symposium Proceedings*, April 14–16, 1998, San Francisco, Belton, D. J., Gaynes, M., Jacobs, E. G., Pearson, R., Wu, T. (Ed.), Materials Research Society, Warrendale, Vol. 515 (1998), pp. 233–238
5. Wiese, S., Feustel, F., Rzepka, S., Meusel, E.: "Creep and Crack Propagation in Flip Chip SnPb37 Solder Joints". *Proc. 49th Electronic Components and Technology Conference*, San Diego, CA, June 1–4, 1999, pp. 1015–1020
6. Zhengfang Qian, Jian Yang, and Sheng Liu: "Visco-Elastic-Plastic Properties and Constitutive Modeling of Underfills". *Proc. 48th Electronic Components and Technology Conference*, Seattle, WA, May 25–28, 1998, pp. 969–974
7. Feustel, F., Vogel, D., Wiese, S.: "Load Free Determination of the Coefficient of Thermal Expansion on Polymer Foils".

*Proc. Micro Materials '97*, Berlin, April 16–18, 1997, pp. 772–775

8. Feustel, F., Eckebracht, A.: "Influence of flux selection and underfill selection on the reliability of flip chips on FR-4". *Proc. 49th Electronic Components and Technology Conference*, San Diego, CA, June 1–4, 1999, pp. 583–588
9. Rzepka, S., Feustel, F., Meusel, E.: The Effect of Underfill Imperfections on the Reliability of Flip Chip Modules: FEM Simulations and Experiments. *Proc. 48th Electronic Components and Technology Conference*, Seattle, WA, May 25–28, 1998, pp. 362–370